

Directed Manipulation of a Flavoprotein Photocycle **

Heike Staudt, Michael Georg Hoesl, Andreas Dreuw, Sascha Serdjukow, Dieter Oesterhelt, Nediljko Budisa, Josef Wachtveitl,* and Martin Grininger*

We have recently characterized the role of the riboflavin-binding protein (RfBP) dodecin from *Halobacterium salinarum* as clearing free riboflavin from the cytoplasm with riboflavin protein dissociation constants in the low nanomolar range,^[1] and as providing riboflavin as the direct precursor for FMN and FAD biosynthesis. To prevent cellular damage, dodecin seals riboflavin in deeply buried binding cavities and neutralizes riboflavin reactivity by extensively quenching photoactivated states.^[2] Both properties are achieved by a remarkable binding mode. Binding to dodecin, riboflavin aligns into a sandwich of aromatic systems in which extensive stacking compensates for minimal hydrogen bonding (Figure 1). In the key step of the relaxation process of the

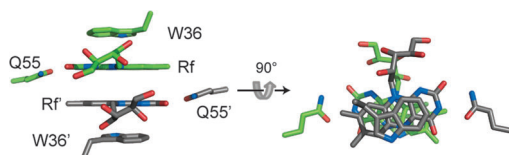


Figure 1. Sandwich-like incorporation of flavins. In dodecin, dimers of riboflavin (Rf) are bound between tryptophans (W36) and aligned antiparallelly by glutamines (Q55) at the interface of two protomers related by C_2 symmetry.

light-activated riboflavin, an electron of tryptophan W36 is transferred to the excited flavin, generating a charge-separated intermediate state that subsequently recombines to the ground state. Recently, we were able to assign time constants

to the individual processes in the photocycle of dodecin: 1) charge separation faster than the resolution of the experiment (<0.2 ps, τ_1); 2) electron back-transfer with a time constant of 0.9 ps (τ_2); (3) a relaxation process with 6 ps parallel to (2) with an intermediate absorbing at 500 nm (τ_3); and (4) proton transfer from the surrounding water coupled with the electron-transfer/back-transfer cycle (Scheme 1).^[3] Based on high-resolution X-ray structural data and a concise functional characterization, establishing a system of extraordinarily well-defined structure–function relationships, we considered dodecin as excellently suited for modulating biological electron-transfer reactions by rational protein design, thereby studying the protein in a manipulative manner.

This approach should be achieved by exchanging the native W36 with analogues of varying ionization potential leading to W36–riboflavin pairs of modulated redox potential difference. Given the computed value of 7.42 eV for the indole unit of tryptophan at the DFT/B3LYP/6-31G* level of theory in the gas phase,^[4] we chose the derivatives 4-amino-tryptophan (4NH₂-W), 4-fluorotryptophan (4F-W), and 4-azatryptophan (4Aza-W) for shifting the ionization potential to 6.68, 7.49, and 7.96 eV, respectively (see Supporting Information). The C-4 position of the flavin-holding W36 was chosen for derivatization, as X-ray structural analysis indicated an empty bulge in the binding pocket allowing non-invasive modification. To prepare noncanonical W36-modified dodecin analogues, we applied the supplementation-based incorporation method (SPI)^[5] together with the established procedures for dodecin purification and folding

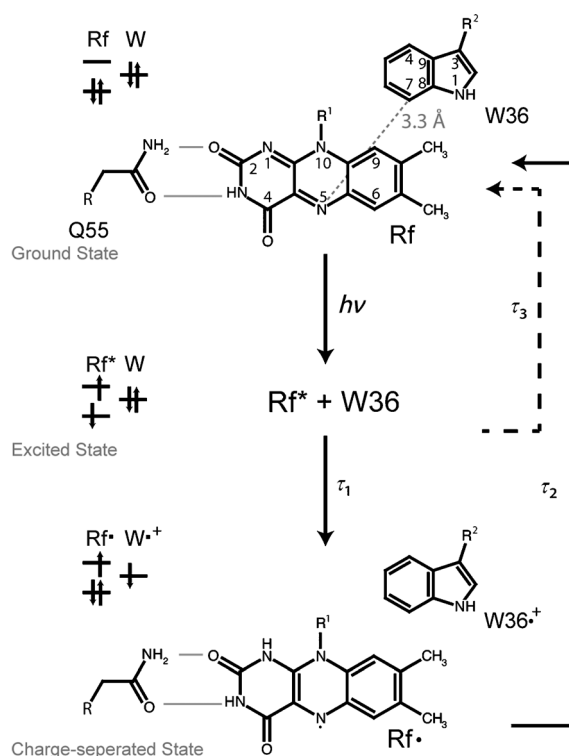
[*] Dr. H. Staudt,^[‡] Prof. Dr. J. Wachtveitl
Institut für Physikalische und Theoretische Chemie, Exzellenzcluster
“Makromolekulare Komplexe”, Goethe Universität Frankfurt
Max-von-Laue-Strasse 7, 60438 Frankfurt am Main (Germany)
E-mail: wweilt@theochem.uni-frankfurt.de
Dr. M. G. Hoesl,^[‡] Prof. Dr. N. Budisa
AK Biokatalyse, Institut für Chemie, Technische Universität Berlin
Müller-Breslau-Strasse 10, 10623 Berlin (Germany)
Prof. Dr. A. Dreuw
Interdisziplinäres Zentrum für wissenschaftliches Rechnen
Ruprecht-Karls Universität
Im Neuenheimer Feld 368, 69120 Heidelberg (Germany)
S. Serdjukow, Prof. Dr. D. Oesterhelt, Prof. Dr. M. Grininger
Abteilung für Membranbiochemie
Max-Planck-Institut für Biochemie
Am Klopferspitz 18, 82152 Martinsried (Germany)
Prof. Dr. M. Grininger
Present address: Institut für Organische Chemie und Chemische
Biologie, Buchmann Institut für Molekulare Lebenswissenschaften
Exzellenzcluster “Makromolekulare Komplexe”

Goethe Universität Frankfurt
Max-von-Laue-Strasse 15, 60438 Frankfurt am Main (Germany)
E-mail: grininger@chemie.uni-frankfurt.de
S. Serdjukow
Present address: Department Chemie und Pharmazie
Ludwig-Maximilians-Universität München
Butenandtstrasse 5–13, 81377 München (Germany)

[‡] These authors contributed equally to this work.

[**] We thank the beamline scientists of the European Synchrotron
Radiation Facility (ESRF) for their assistance during data collection.
We also thank the core facility of the Max-Planck-Institute of
Biochemistry, particularly Lissy Weyher-Stingl, for ESI-MS data
collection of noncanonical dodecins. This work was supported by
the Volkswagen Foundation (Lichtenberg Grant to M.G.), by the
DFG (SFB 807 to H.S. and J.W., and UniCat Cluster of Excellence of
TU Berlin to N.B.), and by the BMBF (Biofuture Grant to N.B.).

Supporting information for this article is available on the WWW
under <http://dx.doi.org/10.1002/anie.201302334>.



(Supporting Information, Tables S1 and S2, Figures S1–S3, for experimental details, see also the Supporting Information).^[1b] We further crystallized dodecin analogues and refined atomic models at 1.7 (4NH₂-W36 dodecin), 1.8 (4F-W36), and 2.0 Å (4Aza-W36) (Supporting Information, Table S3 and experimental details).

The high-resolution X-ray data reveal that the structures of noncanonical versus wild-type dodecins are essentially unchanged. In 4F-W36 and 4NH₂-W36 dodecin, riboflavin finds a slightly deeper position in the binding pocket, as compared to riboflavin in wild-type dodecin, while riboflavin in 4Aza-W36 dodecin is less deeply incorporated. Similarly, C-4-modified W36 vary only marginally in position, essentially in a similar manner as the respective ligands (Figure 2A; Supporting Information, Figure S4). Structures aligned by the indole submoiety of W36 highlight the conserved relative positioning within the photochemically relevant W36-riboflavin couple, and document the non-invasive character of our approach (Figure 2B). The positional changes are significantly less-pronounced than in wild-type dodecin carrying the different flavin cofactors lumiflavin, FMN and FAD. In a previous work where we had charac-

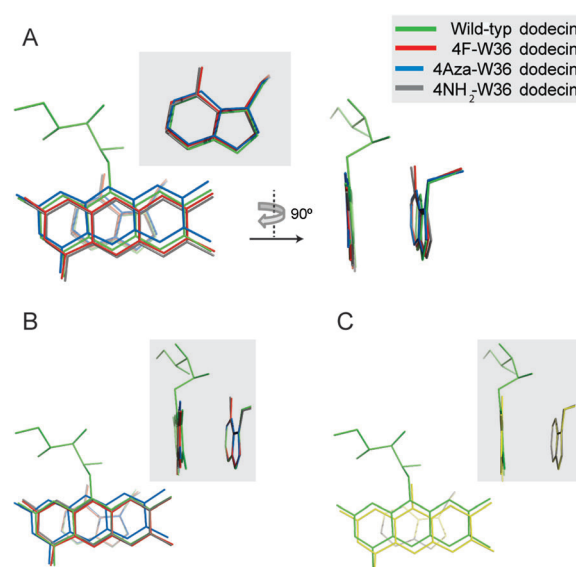


Figure 2. Superposition of W36 and riboflavin in noncanonical dodecin analogues versus wild-type dodecin. A), B) Structures were aligned by C α -backbones (A), and by the indole submoiety of W36 (B). Riboflavins of the noncanonical analogues are represented by their aromatic moieties (isoalloxazine; Supporting Information, Figure S4). In the W36-aligned structure, the riboflavin N-10 atoms are displaced from wild-type dodecin by 0.44 Å (4Aza-W36 dodecin), 0.22 Å (4F-W36), and 0.19 Å (4NH₂-W36). C) Superposition of W36-aligned dodecins with riboflavin (green) and lumiflavin (yellow) as ligands. Lumiflavin N-10 is displaced by 0.52 Å from riboflavin N-10. Atomic coordinates of pdb entry codes 2ccb and 2ccc were used for wild-type dodecin with bound riboflavin and lumiflavin, respectively.^[2b]

terized wild-type dodecin in complex with the different flavins, we did not find spectral differences in transient data, and thus we assume that the even smaller structural changes in noncanonical dodecin analogues similarly do not affect spectroscopic properties (Figure 2C).^[3] In other words, we use a series of highly isomorphous dodecins that only differ in the electronic properties modulated by the ionization potential of W36.

Analysis of the photochemical properties of noncanonical dodecins was performed by transient absorption spectroscopy.^[3] As depicted in Figure 3A, the pattern of negative (blue) and positive (red) absorbance changes differed significantly compared to wild-type dodecin. Most significantly, the negative signal at shorter wavelength (450 nm), describing ground-state bleaching (GB), varies in all noncanonical analogues, and the positive signal at 550–700 nm is dramatically reduced in 4NH₂-W36 dodecin. The positively charged tryptophan radical contributes to absorption around 600 nm,^[6] and consequently the changed spectroscopic properties of tryptophan radicals by C-4 modifications hamper interpretation of transient data at long wavelengths. In contrast, the absorption around 450 nm, which is solely contributed by riboflavin, provides a direct measure for the electronic environment of riboflavins in the dodecin analogues. Accordingly, recovery of GB at 456 nm was used as a readout for the electron back transfer from the riboflavin semiquinone to the positively charged tryptophan radical (see the process described by τ_2 in Scheme 1). Unimolecular

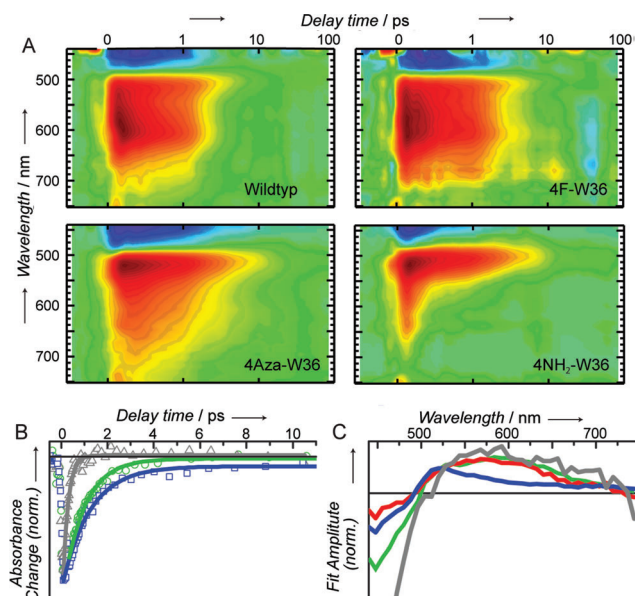


Figure 3. Transient spectroscopic characterization of wild-type dodecin and its noncanonical analogues. Data in (B) and (C) are shown according to the color code of Figure 2. A) Excitation of wild-type dodecin and noncanonical analogues at 388 nm with sapphire white light as the probing pulse. Positive absorbance changes are shown in red and negative changes in blue. The timescale is linear from -0.5 to 1 ps and logarithmic for longer times. B) Transient absorbance change at 456 nm for wild-type, 4Aza-W36 (blue), and 4NH_2 -W36 dodecin (gray). Data for the first 10 ps can be described by a first-order exponential decay. C) Decay-associated spectra of the time constant τ_2 from the global fit analysis of wild-type dodecin and noncanonical analogues (4F-W36 dodecin in red). Spectra are normalized to the absorbance at 388 nm in the static spectra.

recovery rates were fitted to 0.2 , 1.2 , and 0.9 ps for 4NH_2 -W36, 4Aza-W36, and wild-type dodecin, respectively (Figure 3B); thus, the amino substituent of 4NH_2 -W36 dodecin shortens the lifetime of the charge-separated state by a factor of 4, while this intermediate lives slightly longer in the 4Aza-W36 modification (factor 1.3). Data of 4F-W36 dodecin were not fitted owing to a low signal-to-noise ratio. However, the lifetime of the charge-separated state can be estimated to values similar as recorded for wild-type dodecin (Figure 3A), which agrees with the similar ionization potentials of 4F-W and tryptophan.

As for wild-type dodecin, the time-resolved spectroscopic data for the noncanonical dodecin analogues were approximated by global fit analysis.^[3] Except for 4NH_2 -W36 dodecin, four time constants were sufficient to describe the dynamic data (for a thorough analysis of transient spectroscopic data, see the Supporting Information). In a previous study, τ_2 was attributed to describing the back electron transfer, and as such reflects a suited measure for evaluating our approach on the manipulation of electron transfer rates. τ_2 was fitted to 0.9 ps for wild-type dodecin,^[3] and changed to 0.8 for 4F-W36 dodecin, 0.9 for 4Aza-W36 dodecin, and 0.13 for 4NH_2 -W36 dodecin (Figure 3C), indicating that back electron transfer is significantly shortened in 4NH_2 -W36 dodecin (by a factor of 7), which is consistent with the obtained unimolecular recovery rates (Figure 3B). Overall, similar signatures for τ_2

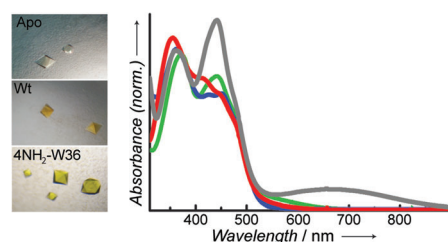


Figure 4. Static absorption spectra of noncanonical dodecins. Absorption differences at 350 – 500 nm indicate differences in the $S_0 \rightarrow S_1$ and $S_0 \rightarrow S_2$ transitions of bound riboflavins. In addition, 4NH_2 -W36 dodecin exhibits long wavelength absorption due to charge-transfer complex formation leading to greenish-colored protein, as shown by images of protein crystals. Crystals are depicted as grown in their mother liquor; Wt = wild-type dodecin with bound riboflavin, Apo = wild-type apododecin, 4NH_2 -W36 = 4NH_2 -W36-dodecin.

imply an essentially unchanged photochemistry in wild-type dodecin and its noncanonical analogues (Figure 3C). The differences in τ_2 signatures are most likely caused by different static spectral characteristics of the positively charged tryptophan radical absorbing at 550 – 600 nm, as already stated above.

As another particularity for 4NH_2 -W36 dodecin, we found a broad absorption band at 650 nm (Figure 4). This is reminiscent to early studies on the flavoprotein D-amino acid oxidase with incorporated aminobenzoate ligands, where long wavelength absorption was explained on the basis of charge-transfer complex formation.^[7] This interpretation is in line with the low ionization potential of 4NH_2 -W, and may also depend on the geometry of the 4NH_2 -W36-riboflavin couple. Induction of a long-wavelength charge-transfer transition band by stable amino modifications of aromatic amino acids in close vicinity to the flavin ligand is potentially interesting, as it can make flavin photochemistry available to red-light absorption.

In wild-type dodecin, the initial electron transfer from the tryptophan to the excited flavin occurs in less than 0.2 ps (time resolution of the experiment), followed by charge recombination with a time constant of 0.9 ps. Owing to the high ΔG^0 value of approximately -1.95 eV, the back electron transfer is expected to be in the inverted Marcus region (Figure 5).^[2b,8] The higher ionization potential of 4-azaindole

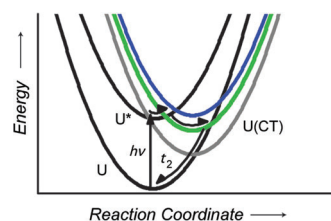


Figure 5. Potentials of the involved states. The potentials of dodecins are modeled in the ground (U) and excited state (U^*), as indicated by black lines. Charge-separated-state potentials ($U(\text{CT})$) of wild-type, 4Aza-W36, and 4NH_2 -W36 dodecin are estimated by the ionization potentials of riboflavin, W36, and the differences in the ionization energies between indole and the corresponding indole derivatives. The reorganization energy was estimated to be 1 eV. The ionization energy of 4F-indole is close to indole, and is not depicted.

leads to an increased potential of the charge-separated state in 4Aza-W36 dodecin, and thus ΔG^0 is higher for the electron back transfer, resulting in slowed reaction rates for the back transfer. Consistently, based on the decreased potential of the charge-separated state and its lowered ΔG^0 , electron back transfer in 4NH₂-W36 dodecin is faster than in the wild-type protein (Figure 5).

By using dodecin modified by specific and subtle chemical modifications in the important amino acid W36, we have demonstrated that electron transfer processes of a flavoprotein photocycle can be selectively manipulated in a controllable manner. This is a system with minimal structural perturbations, as documented by high-resolution X-ray structures, which enabled us to obtain transient spectroscopic data that fully confirmed quantum-chemically predicted changes of electron transfer rates. In a broader context, we present a case study from an ideal situation in which knowledge and methods from different disciplines can be integrated to rationally engineer single parameters in otherwise non-perturbed complex systems.

Received: March 19, 2013

Published online: July 1, 2013

Keywords: bioorganic chemistry · electronic structure · flavins · photochemistry · proteins

- [1] a) B. Bieger, L. O. Essen, D. Oesterhelt, *Structure* **2003**, *11*, 375–385; b) M. Grininger, K. Zeth, D. Oesterhelt, *J. Mol. Biol.* **2006**, *357*, 842–857; c) M. Grininger, H. Staudt, P. Johansson, J. Wachtveitl, D. Oesterhelt, *J. Biol. Chem.* **2009**, *284*, 13068–13076.
- [2] a) N. Mataga, H. Chosrowjan, S. Taniguchi, F. Tanaka, N. Kido, M. Kitamura, *J. Phys. Chem. B* **2002**, *106*, 8917–8920; b) D. Zhong, A. H. Zewail, *Proc. Natl. Acad. Sci. USA* **2001**, *98*, 11867–11872.
- [3] H. Staudt, D. Oesterhelt, M. Grininger, J. Wachtveitl, *J. Biol. Chem.* **2012**, *287*, 17637–17644.
- [4] a) R. G. Parr, W. Yang, *Density Functional Theory of Atoms and Molecules*, Oxford University Press, New York, **1989**; b) A. D. Becke, *J. Chem. Phys.* **1993**, *98*, 5648–5652; c) Y. Shao, L. F. Molnar, Y. Jung, J. Kussmann, C. Ochsenfeld, S. T. Brown, A. T. B. Gilbert, L. V. Slipchenko, S. V. Levchenko, D. P. O'Neill, R. A. DiStasio, Jr., R. C. Lochan, T. Wang, G. J. O. Beran, N. A. Besley, J. M. Herbert, C. Y. Lin, T. Van Voorhis, S. H. Chien, A. Sodt, R. P. Steele, V. A. Rassolov, P. E. Maslen, P. P. Korambath, R. D. Adamson, B. Austin, J. Baker, E. F. C. Byrd, H. Dachsel, R. J. Doerksen, A. Dreuw, B. D. Dunietz, A. D. Dutoi, T. R. Furlani, S. R. Gwaltney, A. Heyden, S. Hirata, C.-P. Hsu, G. Kedziora, R. Z. Khallilulin, P. Klunzinger, A. M. Lee, M. S. Lee, W. Liang, I. Lotan, N. Nair, B. Peters, E. I. Proynov, P. A. Pieniazek, Y. M. Rhee, J. Ritchie, E. Rosta, C. D. Sherrill, A. C. Simmonett, J. E. Subotnik, H. L. Woodcock III, W. Zhang, A. T. Bell, A. K. Chakraborty, D. M. Chipman, F. J. Keil, A. Warshel, W. J. Hehre, H. F. Schaefer III, J. Kong, A. I. Krylov, P. M. W. Gill, M. Head-Gordon, *Phys. Chem. Chem. Phys.* **2006**, *8*, 3172–3191.
- [5] N. Budisa, B. Steipe, P. Demange, C. Eckerskorn, J. Kellermann, R. Huber, *Eur. J. Biochem.* **1995**, *230*, 788–796.
- [6] S. Solar, N. Getoff, P. S. Surdhar, D. A. Armstrong, A. Singh, *J. Phys. Chem.* **1991**, *95*, 3639–3643.
- [7] a) V. Massey, H. Ganther, *Biochemistry* **1965**, *4*, 1161–1173; b) R. Miura, C. Setoyama, Y. Nishina, K. Shiga, H. Mizutani, I. Miyahara, K. Hirotsu, *J. Biochem.* **1997**, *122*, 825–833; c) J. H. Bae, M. Rubini, G. Jung, G. Wiegand, M. H. Seifert, M. K. Azim, J. S. Kim, A. Zumbusch, T. A. Holak, L. Moroder, R. Huber, N. Budisa, *J. Mol. Biol.* **2003**, *328*, 1071–1081.
- [8] R. Marcus, N. Sutin, *Biochim. Biophys. Acta* **1985**, *811*, 265–322.